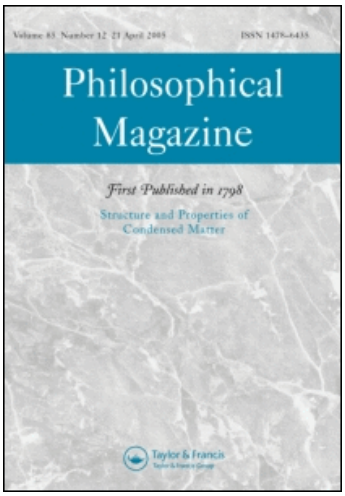

Philosophical Magazine
Publication details, including instructions for authors and subscription information:
http://www.informaworld.com/smpp/title~content=t713695589

Simulation of the dynamics of hard ellipsoids

C. de Michele [a]; R. Schilling [b]; F. Sciortino [a]
[a] INFM-CRS Soft and Dipartimento di Fisica, Università di Roma 'La Sapienza', Roma, Italy [b] Johannes-Gutenberg-Universitat Mainz, Mainz, Germany

Online Publication Date: 01 November 2008

To cite this Article de Michele, C., Schilling, R. and Sciortino, F.(2008)'Simulation of the dynamics of hard ellipsoids',Philosophical Magazine,88:33,4117 — 4123
To link to this Article: DOI: 10.1080/14786430802537761
URL: http://dx.doi.org/10.1080/14786430802537761

Philosophical Magazine
Vol. 88, Nos. 33–35, 21 November–11 December 2008, 4117–4123

Taylor & Francis
Taylor & Francis Group

Simulation of the dynamics of hard ellipsoids

C. de Michele[a]*, R. Schilling[b] and F. Sciortino[a]

[a]*INFM-CRS Soft and Dipartimento di Fisica, Università di Roma 'La Sapienza', Roma, Italy;*
[b]*Johannes-Gutenberg-Universitat Mainz, Mainz, Germany*

(*Received 26 May 2008; final version received 3 October 2008*)

We study a system of uniaxial hard ellipsoids by molecular dynamics simulations, changing both the aspect-ratio X_0 ($X_0 = a/b$, where a is the length of the revolution axis and b is the length of the two other axes) and the packing fraction ϕ. We calculate the translational $\langle r^2(t)\rangle$ and rotational $\langle \Phi^2(t)\rangle$ mean squared displacements, the translational $D_{\rm trans}$ and the rotational $D_{\rm rot}$ diffusion coefficients and the associated isodiffusivity lines in the $\phi - X_0$ plane. For the first time, we characterize the cage effect through the logarithmic time derivative of $\log\langle r^2(t)\rangle$ and $\log\langle \Phi^2(t)\rangle$. These quantities exhibit a minimum if the system is supercooled and we show that, consistently with our previous findings, for large and small X_0 values, rotations are supercooled, contrary to translations. In agreement with this scenario, while the self-intermediate scattering function exhibits stretched relaxation (i.e. glassy dynamics) only for large ϕ and $X_0 \approx 1$, the second order orientational correlator $C_2(t)$ show stretching only for large and small X_0 values. As further evidence of this pre-nematic order driven glass transition, we observe a decoupling of the translational and rotational dynamics, which generates an almost perpendicular crossing of the $D_{\rm trans}$ and $D_{\rm rot}$ isodiffusivity lines.

Keywords: computer simulation; glass transition; hard ellipsoids; mode coupling theory; nematic order

1. Introduction

Even if particles interact with only excluded volume interactions, they may exhibit a rich phase diagram; for example, it is known that simple non-spherical hard-core particles can form either crystalline or liquid crystalline ordered phases [1], as first shown analytically by Onsager [2] for rod-like particles. Accurate phase diagrams of several hard-body shapes can be found in the literature [3–6], but detailed information about dynamics properties and kinetically arrested states of hard-core bodies are not available. While mode coupling theory (MCT) [7] effectively describes the slowing down of the dynamics of a hard-sphere system on increasing the packing fraction ϕ, its molecular counterpart, the molecular model coupling theory (MMCT) [8], has not been tested in simulated or real systems yet. On going from spheres to non-spherical particles, non-trivial phenomena arise, due to the interplay between translational and rotational degrees of freedom. The slowing down of the dynamics can indeed appear either in both translational and rotational properties or in

*Corresponding author. Email: cristiano.demichele@roma1.infn.it

ISSN 1478–6435 print/ISSN 1478–6443 online

DOI: 10.1080/14786430802537761
http://www.informaworld.com

just one of the two. Hard ellipsoids (HE) of revolution [1,9] are one of the most prominent systems composed of hard body anisotropic particles, and MMCT has been applied to HE [10,11], predicting a swallow-like glass transition line. In addition, the theory suggests that for $X_0 \lessapprox 0.5$ and $X_0 \gtrapprox 2$, the glass transition is driven by a precursor of nematic order, resulting in an orientational glass where the translational density fluctuations are quasi-ergodic, except for very small wave vectors q.

2. Methods

We perform an extended study of the dynamics of monodisperse HE in a wide window of ϕ and X_0 values, extending the range of X_0 previously studied [12].

We study the translational and rotational mean squared displacements, looking for evidence of the cage effect and the translational and rotational correlation functions, to search for the onset of slowing down and stretching in the decay of the correlation. We also focus on establishing the trends leading to dynamic slowing down in both translations and rotations, by evaluating the loci of constant translational and rotational diffusion. These lines, in the limit of vanishing diffusivities, approach the glass-transition lines. We simulate a system of $N = 512$ ellipsoids at various volumes $V = L^3$ in a cubic box of edge L with periodic boundary conditions. We chose the geometric mean of the axis $l = \sqrt[3]{ab^2}$ as the unit of distance, the mass m of the particle as the unit of mass ($m = 1$) and $k_B T = 1$ (where k_B is the Boltzmann constant and T is the temperature), and hence the corresponding unit of time is $\sqrt{ml^2/k_B T}$. The inertia tensor is chosen as $I_x = I_y = 2mr^2/5$, where $r = \min\{a, b\}$. The value of the I_z component is irrelevant [13], since the angular velocity along the symmetry (z-) axis of the HE is conserved. We simulate a grid of more than 500 state points at different X_0 and ϕ. To create the starting configuration at a desired ϕ, we generate a random distribution of ellipsoids at very low ϕ and then we progressively decrease L to the desired ϕ. We then equilibrate the configuration by propagating the trajectory for times such that both angular and translational correlation functions have decayed to zero. Finally, we perform a production run at least 30 times longer than the time needed to equilibrate. For the points close to the isotropic-nematic (I-N) transition, we check the nematic order by evaluating the largest eigenvalue S of the order tensor (for further details see [14]).

3. Results and discussion

3.1. *Mean squared displacements*

A first characterization of HE dynamics is offered by translational and rotational mean squared displacements (MSD). Translational MSD is defined as

$$\langle r^2(t) \rangle = \frac{1}{N} \sum_i \langle \| \mathbf{x}_i(t) - \mathbf{x}_i(0) \|^2 \rangle, \tag{1}$$

where N is the number of HE, and $\mathbf{x}_i(t)$ is the position of the centre-of-mass of the i-th HE. Analogously the rotational MSD is

$$\langle \Phi^2(t) \rangle = \frac{1}{N} \sum_i \langle \| \Delta \Phi_i \|^2 \rangle, \tag{2}$$

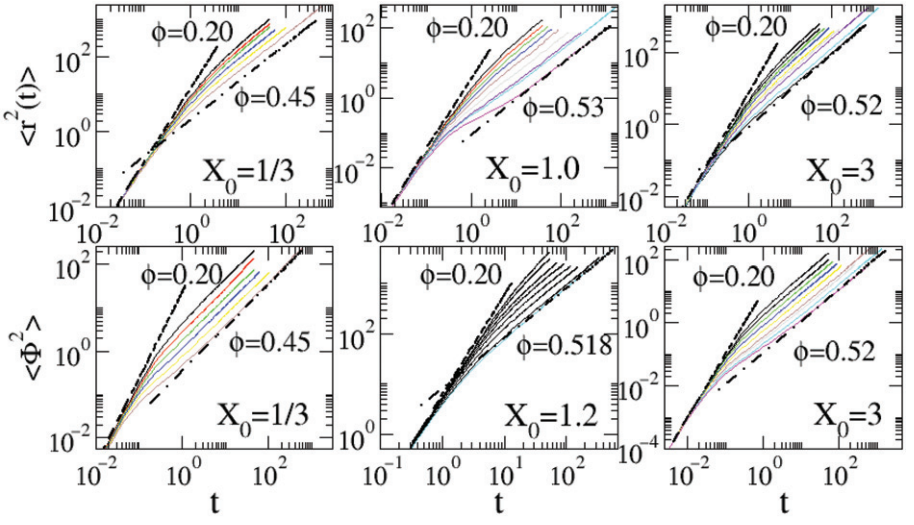

Figure 1. (Colour online). Translational (top) and rotational (bottom) MSD for three different elongations at different volume fractions. Top (from left to right) $X_0 = 1/3$ (from top to bottom: $\phi = 0.20 \ldots 0.45$), 1.0 ($\phi = 0.20 \ldots 0.53$), 3.0 ($\phi = 0.20 \ldots 0.52$). Bottom (from left to right): $X_0 = 1/3$ ($\phi = 0.20 \ldots 0.45$), 1.2 ($\phi = 0.20 \ldots 0.518$), 3.0 ($\phi = 0.20 \ldots 0.52$). Dashed lines and dot-dashed lines are guides to the eye, showing the ballistic and diffusive regime, respectively.

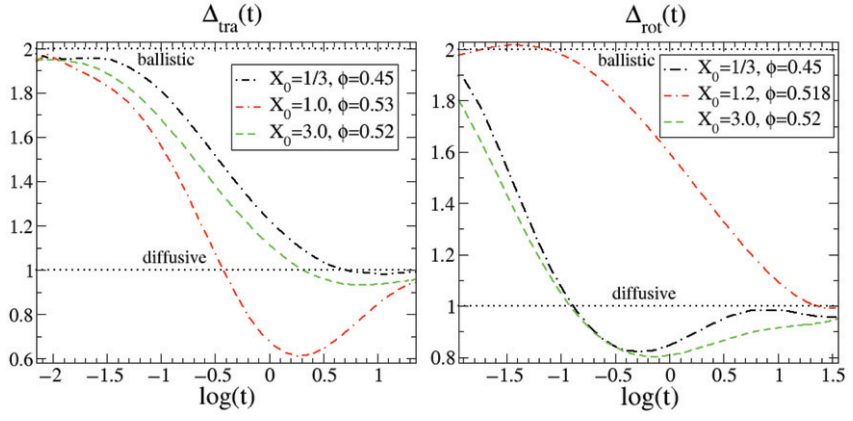

Figure 2. (Colour online). $\Delta_{tra}(t)$ and $\Delta_{rot}(t)$ (see text for their definitions) for the most 'supercooled' state points simulated for four different elongations. Dotted lines indicate the ballistic and diffusive regimes.

where $\Delta\Phi_i = \int_0^t \omega_i \mathrm{d}t$, ω_i being the angular velocity of the i-th HE. In Figure 1, translational and rotational MSD are reported for three different elongations at different volume fractions. Both translational and rotational MSD shows for short times a ballistic regime, where $\langle r^2(t)\rangle$, $\langle \Phi^2(t)\rangle \propto t^2$, which crosses over to a diffusion process at long times; i.e. $\langle r^2(t)\rangle$, $\langle \Phi^2(t)\rangle \propto t$. For the state points simulated in the present study, for $\langle \Phi^2 \rangle$ the ballistic short-time and the diffusive long-time regimes are separated by an intermediate

time window, due to particles caging, only for high elongations; i.e. for $X_0 = 1/3$ and $X_0 = 3$ in Figure 1. In contrast, for $\langle r^2 \rangle$ this intermediate regime shows up only for elongations close to 1. The scenario just depicted is more apparent if we consider the quantities: $\Delta_{tra}(t) = \partial \log(\langle r^2(t) \rangle)/\partial \log t$ and $\Delta_{rot}(t) = \partial \log(\langle \Phi^2(t) \rangle)/\partial \log t$ (see Figure 2). The short- and the long-time limits of $\Delta_{tra}(t)$, $\Delta_{rot}(t)$ correspond to the ballistic ($\Delta_{tra}(0)$, $\Delta_{rot}(0) = 2$) and the diffusive regimes ($\Delta_{rot}(\infty)$, $\Delta_{rot}(\infty) = 1$), respectively. Anyway, if the translational, or rotational, velocity autocorrelation function (VCF) exhibits a negative tail at long times, $\Delta_{tra}(t)$ shows a minimum. In other words, a monotonically decreasing translational (rotational) VCF, that is without the cage effect, corresponds to a monotonically decreasing $\Delta_{tra}(t)$ ($\Delta_{rot}(t)$)[15].

3.2. *Orientational correlation function*

The cage effect of $\langle \Phi^2(t) \rangle$ for large X_0, approaching the nematic phase, supports the possibility of a close-by glass transition. To further support this possibility we evaluate the self part of the intermediate scattering function $F_{self}(q, t) = \frac{1}{N} \langle \sum_j e^{i \cdot (\mathbf{x}_j(t) - \mathbf{x}_j(0))} \rangle$ and the second order orientational correlation function $C_2(t)$, defined as [12] $C_2(t) = \langle P_2(\cos\theta(t)) \rangle$, where $P_2(x) = (3x^2 - 1)/2$ and $\theta(t)$ is the angle between the symmetry axis at time t and at time 0. The over-compressing, achievable for HE, is rather limited (as for the well known hard-sphere case), nevertheless rotational and translational correlation functions reveal that the onset of dynamic slowing down and glassy dynamics can be detected by the appearance of stretching. F_{self} shows exponential behavior close to the I-N transition ($X_0 = 3.2, 0.3448$) on the prolate and oblate side, and only when $X_0 \approx 1$, does F_{self} develop a small stretching, consistent with the minimum of the swallow-like curve observed in the fluid–crystal line [16,17], in the jamming locus as well as in the predicted behavior of the glass line for HE [8] and for small elongation dumbbells [18,19].

In contrast to the F_{self} behavior, the orientational correlation function C_2 shows stretching at large anisotropy (i.e. at small and large X_0 values), but decays within the microscopic time for almost spherical particles, in accordance with the cage effect of $\langle \Phi^2(t) \rangle$. Previous studies of the rotational dynamics of HE [12] did not report stretching in C_2, probably due to the smaller values of X_0 previously investigated, and to the present increased statistic, which allows us to follow the full decay of the correlation functions.

In summary, C_2 becomes stretched approaching the I-N transition, while F_{self} remains exponential on approaching the transition. To quantify the amount of stretching in C_2, we fit it to the function $A \exp[-(t/\tau_{C_2})^{\beta_{C2}}]$ (stretched exponential) for several state points and we show in Figure 3 the X_0 dependence of τ_{C_2} and β_{C_2} for three different values of ϕ. In all cases, slowing down of the characteristic time and stretching increases progressively on approaching the I-N transition.

3.3. *Isodiffusivity lines*

For all the simulated state points, we evaluated the translational (D_{trans}) and rotational (D_{rot}) diffusion coefficients. Then, by proper interpolation of D_{trans} and D_{rot}, we evaluate the corresponding isodiffusivity lines, which are the loci of points, in the X_0-ϕ diagram, having the same diffusivity. Isodiffusivity lines are shown in Figure 4. What emerges clearly from this figure is a striking decoupling of the translational and rotational

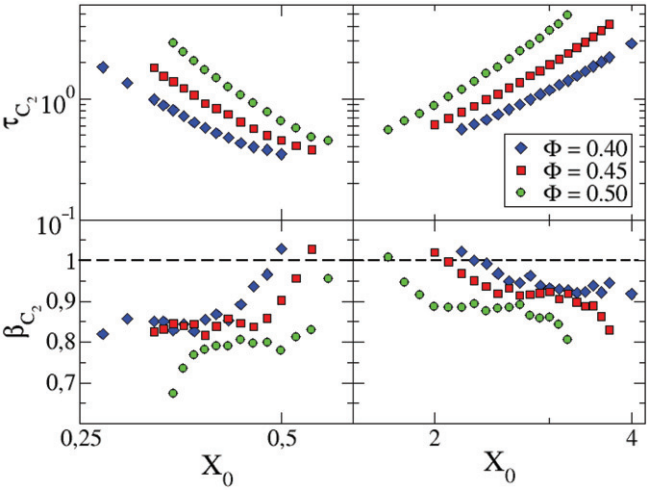

Figure 3. (Colour online). β_{C_2} and τ_{C_2} are obtained from fits of C_2 to a stretched exponential for $\phi = 0.40$, 0.45 and 0.50. Top: τ_{C_2} as a function of X_0. Bottom: β_{C_2} as a function of X_0. The time window used for the fits is chosen in such a way to exclude the microscopic short-time ballistic relaxation. For $0.588 < X_0 < 1.7$ the orientational relaxation is exponential.

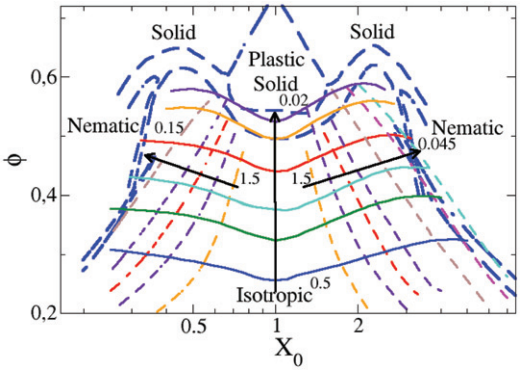

Figure 4. (Colour online). Isodiffusivity lines. Solid lines are isodiffusivity lines from translational diffusion coefficients D_{trans}, and dashed lines are isodiffusivities lines from rotational diffusion coefficients D_{rot}. Arrows indicate decreasing diffusivities. Left and right arrows refer to rotational diffusion coefficients. Diffusivities along the left arrow are 1.5, 0.75, 0.45, 0.3, 0.15. Diffusivities along the right arrow are 1.5, 0.75, 0.45, 0.3, 0.15, 0.075, 0.045. The central arrow refers to translational diffusion coefficients, whose values are 0.5, 0.3, 0.2, 0.1, 0.04, 0.02. The thick long-dashed curves are coexistence curves of all first order phase transitions in the phase diagram of HE, evaluated by Frenkel and Mulder [20]. Solid lines are coexistence curves for the I-N transition of oblate and prolate ellipsoids, obtained analytically by Tijpto-Margo and Evans [6].

dynamics: translational isodiffusivity lines resemble the swallow-like shape of the coexistence between the isotropic liquid and crystalline phases (as well as the MMCT prediction for the glass transition [8]), while rotational isodiffusivity lines have qualitatively the same shape as the I-N coexistence curve.

Translation isodiffusivity lines run almost parallel to the x-axis, i.e. translational diffusion is mainly controlled by volume fraction (packing), that is the y-axis in Figure 4. In contrast, due to the almost perpendicular crossing of translational and rotational isodiffusivity lines, the rotational isodiffusivity lines are instead mostly controlled by X_0, showing a progressive slowing down of the rotational dynamics independent from the translational behavior. In other words, moving along a translational isodiffusivity path, D_{rot} progressively decreases until the rotational diffusion is completely arrested. Unfortunately, in our specific case of monodisperse HE, before reaching this point the I-N nematic instability intervenes, and we were able to observe only a limited degree of supercooling. It would be intriguing to design a system of hard particles, where the nematic transition is completely inhibited. Likely this system can be obtained by a proper choice of the disorder in the particle's shape and/or elongations. MMCT predicts a nematic glass for large X_0 HE [8], in which orientational degrees of freedom start to freeze approaching the isotropic-nematic transition line, while translational degrees of freedom mostly remain ergodic. Hence, our slowing down of the rotational dynamics is consistent with the results of this theory.

4. Conclusions

In summary we investigated the dynamics properties of a system of monodisperse HE and we have shown that clear precursors of dynamic slowing down, like the stretching of correlation functions and the cage effect, can be observed in the region of the phase diagram where a (meta)stable isotropic phase can be studied. In particular our data suggest, in accordance with MMCT predictions [8], at least two possible glass transition mechanisms: a slowing down in the orientational degrees of freedom (when $X_0 \lessapprox 0.5, X_0 \gtrapprox 2$), driven by the elongation of the particles and related to pre-nematic order (quantitative predictions about precursors effects of I-N transition can be also found in [21] and they can be checked using our data; work on this is under way), and a slowing down in the translational degrees of freedom (active for $0.5 \lessapprox X_0 \lessapprox 2$) driven by packing and related to the cage effect. The main effect of the existence of these two complementary arrest mechanisms is a decoupling of the translational and rotational dynamics which generates an almost perpendicular crossing of the D_{trans} and D_{rot} isodiffusivity lines.

Acknowledgement

We acknowledge support from MIUR-PRIN.

References

[1] M.P. Allen, *Liquid Crystal Systems*, Vol. 23, N. Attig, K. Binder, H. Grubmüller and K. Kremer eds., John von Neumann Institute for Computing, Jülich, 2004, pp.289–320.
[2] L. Onsager, Ann. N. Y. Acad. Sci. 51 (1949) p.627.
[3] J.D. Parsons, Phys. Rev. A 19 (1979) p.1225.
[4] S.D. Lee, J. Chem. Phys. 89 (1989) p.7036.
[5] A. Samborski, G.T. Evans, C.P. Mason et al., Mol. Phys. 81 (1994) p.263.
[6] B. Tijpto-Margo and G.T. Evans, J. Chem. Phys. 93 (1990) p.4254.

[7] W. Götze, *Aspects of Structural Glass Transition*, J.P. Hansen, D. Levesque and J. Zinn-Justin eds., North-Holland, Amsterdam, 1991, pp.287–499.
[8] M. Letz, R. Schilling and A. Latz, Phys. Rev. E 62 (2000) p.5173.
[9] G.S. Singh and B. Kumar, Ann. Phys. 294 (2001) p.24.
[10] T. Franosch, M. Fuchs, W. Götze et al., Phys. Rev. E 56 (1997) p.5659.
[11] R. Schilling and T. Scheidsteger, Phys. Rev. E 56 (1997) p.2932.
[12] M.P. Allen and D. Frenkel, Phys. Rev. Lett. 58 (1987) p.1748.
[13] M.P. Allen, D. Frenkel and J. Talbot, *Molecular Dynamics Simulations Using Hard Particles*, North-Holland, Amsterdam, 1989.
[14] C. De Michele, R. Schilling and F. Sciortino, Phys. Rev. Lett. 98 (2007) pp.265702–1.
[15] L. Larini, A. Ottochian, C. De Michele et al., Nature Phys. 4 (2008) p.42.
[16] P.N. Pusey and W. Megenvan, Phys. Rev. Lett. 59 (1987) p.2083.
[17] W.G. Hoover and F.H. Ree, J. Chem. Phys. 49 (1968) p.3609.
[18] S.H. Chong and W. Götze, Phys. Rev. E 65 (2002) pp.041503–1.
[19] S.H. Chong, A.J. Moreno, F. Sciortino et al., Phys. Rev. Lett. 94 (2005) pp.215701–1.
[20] D. Frenkel and B.M. Mulder, Molec. Phys. 55 (1991) p.1171.
[21] D. Kivelson and T. Keyes, J. Chem. Phys. 57 (1972) p.4599.